VELOCITY DISTRIBUTION MEASUREMENTS OF CESIUM BEAM TUBES

David A. Howe

Frequency & Time Standards Section
National Bureau of Standards
Boulder, Colorado 80302

Abstract

This paper presents the current collection of Cs beam tube velocity distributions using an automated measurement system. The pulse technique of atomic velocity selection is the method incorporated in the system. Measurements were made on tubes used at the U.S. Naval Observatory and at the NBS Boulder Laboratories. The data reveal that analysis of beam optics is directly possible to a high degree. Frequency stability $\sigma_y(\tau)$ is shown for some of the standards with tubes involved in the tests, and correlations between beam distribution features and $\sigma_y(\tau)$ are discussed. Paricular attention is put on the differences in characteristics among tubes at nominal and high temperatures, old versus new tubes, and single beam compared to multi-beam tubes.

Introduction

About five years ago, a method was realized of directly measuring a Cs beam tube atomic velocity distribution by taking advantage of the dual-interaction cavity arrangement which is commonly used [1]. The method calls for the R.F. excitation signal to enter the tube's microwave cavity in precisely timed bursts. The tube will yield a Ramsey spectrum only for those atoms traveling at a velocity such that it is properly excited by both interaction windows. An analogy can be drawn between this method and a mechanical chopper method as shown in Fig. 1. A properly excited atom will have velocity

$$V_k = \frac{L}{nT_k}$$

where L = length between interaction regions,
T_k = kth period of R.F. bursts
and n = integer (1, 2, 3...)

In the commonly encountered case where tube optics limit the high and low velocities, one can assume n = 1 or 2. Furthermore one can unambiguously select velocities with proper synchronous detection of the Ramsey pattern and proper choice of burst width and power [2]. This measurement technique is known as the pulsed method of velocity measurement.

Knowledge of the atomic velocity distribution yields information about the design of the optics in a beam tube. One can accurately judge the effects of mechanical adjustments or environmental influences by noting changes in the distribution or uncommon characteristics. Moreover, one can calculate the frequency offset of the device due to the second-order Doppler effect.

This paper presents velocity distribution measurements which have been made to date. Except for NBS-4 and NBS-6 (laboratory standards at the National Bureau of Standards), all of the distributions were from commercial Cs tubes.

Procedure

A computer-assisted system was built for acquiring velocity distributions virtually automatically. The system provides an R.F. microwave signal to the Cs tube's cavity in programmed burst lengths and over a range of repetition rates. The R.F. power level is also programmed into the system. Besides the cavity connection, the signal from the tube's detector is connected to the system. With the tube operating in the mono-velocity mode, the intensity of the Ramsey spectrum is determined by square-wave modulation between the Ramsey center peak and the first adjacent valley frequencies. A synchronous (or lock-in) demodulator is used to establish the amplitude and the result is recorded on a reel-to-reel tape storage peripheral.

After the system has gathered data over a prescribed range of mono-velocities, each value at V_k is multiplied by T_k (the corresponding k^{th} pulse period) in order to get $\rho(v)$. This multiplication equalizes the data points since long pulse periods make the tube operate with a smaller duty cycle than short pulse periods; therefore, the Ramsey amplitude will necessarily be smaller. After this, $\rho(v)$ is normalized to unity, and one obtains a plot similar to that shown in Fig. 2.

Fig. 3 has plots comparing a typical beam tube distribution as measured at the detector with the kind of distribution one might see out of the oven. In most beam tubes, the oven operates at approximately 90° C. The corresponding most probable velocity is about 2.4×10^4 cm/s. The fact that many tubes show contours in their respective $\rho(v)$ which are substantially different indicates that the resultant velocity distribution is determined at essentially all points by the optics configuration [3].

Data

To date, 17 commercial Cs tubes have been measured using the velocity acquisition system. It takes about one hour to prepare the tube and system for a measurement and about another hour to collect a 40-point plot of the distribution. Most of the tubes were from standards used by the U.S. Naval Observatory, Time Services Division. Many others were from the NBS Boulder Laboratory. In each plot, the R.F. microwave pulse width (τ) and power (P) above optimum power in C.W. mode (P_o) are listed.

The distributions of the NBS primary Cs standards, NBS-4 and NBS-6, were measured and the results are shown in Fig. 4. The plots denoted by "measured $\rho_x(v)$" were those taken using the pulse technique. Also shown on these graphs are velocity distributions which were computed from the Ramsey spectra at different R.F. microwave power settings [4]. Agreement between the measurement of $\rho(v)$ using the pulse technique and the computed distribution based on Ramsey spectra is within 5%.

NBS-4 (Fig. 4) has a length between cavity interaction regions of about 0.5 m and uses off-axis geometry. One notes considerable attenuation of velocities around 2.0×10^4 cm/s. This is principally due to a vane centered in each cavity window, hence the center of the beam cross-section. The addition of the vanes tends to make the tube act like a two-beam configuration.

NBS-6 (Fig. 5) is a long device having a length between interaction regions of 3.74 m. On-axis geometry is used and the positions of detector and oven can be changed along the length and laterally to the beam. Also, beam stops can be positioned along the beam. Fig. 5

shows a velocity distribution taken from NBS-6 for a particular optics configuration. A plot of the distribution based on Ramsey spectra is again included.

The next set of eight figures are distributions from commercial tubes. Figures 6, 9, 10, and 12 are from single-beam tubes. The others in this set employ multiple-beam configurations, and one sees a trend toward more than one peak feature in these plots. This is especially noticeable in Fig. 8. With the tube represented in Fig. 8, two distributions were measured; one is the tube after one hour of warm-up and the other one day warm-up. All of these tubes were in standards showing a history of good stability performance, and the tubes were measured under factory-specified conditions, i.e., normal oven temperature, normal C-field, etc.

Fig. 14 is the velocity distribution of a malfunctioning single-beam tube. The standard was being repaired at the time of the measurement and had been subject to an excessive mechanical blow of some sort. The shock caused the standard to fail to lock properly. The velocity distribution result shows a noticeable departure from the distributions which one commonly sees with this particular tube. One notes considerable broadening around the peak as well as less high-velocity attenuation.

The next set of four figures are distributions from properly operating commercial tubes. All of these tubes are multiple-beam devices except for the one plotted in Fig. 17, a single-beam device. The tube of Fig. 15 shows a pronounced double-peak characteristic again as a result of the superposition of distributions. The slight scattering of points indicated in Fig. 17 was due somewhat to the lower-than-normal signal out of the tube's detector. It was necessary to average the synchronous detector output at each point over a longer time in order to get a reasonably continuous curve.

The next two tubes (Figs. 19 and 20) were older commercial devices having a continuously operating lifetime of about 5 years. They had shown good service records, and long-term stability approached 2×10^{-13} $[\sigma_y(\tau)]$. No obvious abnormalties are evident in the distributions.

One powerful use of the velocity measurement system is in characterizing the ageing process in tubes. With measurements taken at regular intervals over the life of a tube, one can observe changes in the beam as a diagnostic aid. The system will be used again to remeasure many of the tubes measured to see what ageing effects take place.

The last two tubes (Figs. 21 and 22) were operated at an oven temperature which was 12° higher than normally specified. This was done in order to obtain greater signal-to-noise ratio out of the detector so that short-term stability of the standards could be improved. Both were multiple-beam tubes and no radical departures from a normal distribution exist. With the tube of Fig. 22, a velocity distribution was measured with the oven at its normal operating temperature. The fact that one sees a slight increase in the high and low velocity components at a higher oven temperature indicates that the total beam cross-section has increased.

It is instructive to compare the velocity distribution measurements to stability measurements for a given tube operating as a frequency standard. Generally speaking, one can site types of undesirable effects in the beam trajectory as a function of time. The detected signal is dependent upon the mechanical stability of the oven, state-selector magnets, mass-spectrometer and electron multiplier (if any), and ionizer. Furthermore, there is sensitivity to fluctuations in the Cs emission characteristics of the oven. We shall catagorize these types of effects as "beam noise" and will ignore the detected signal sensitivity to R.F. microwave power and power supply fluctuations although they do affect the detected signal.

Velocity distribution measurements using the pulse technique enable direct monitoring of beam noise in a Cs tube to some degree. Beam noise would give rise to fluctuations in the distribution as a function of time. The measurement system computes an average distribution over about a 100 second period per data point. Assuming gaussian noise, the measurement estimate per point should improve with averaging time. Thus, the plots of distributions do not disclose information about beam noise as the plots are presented in this manuscript. However, if one were to make successive measurements over a given averaging time and noted the extent of fluctuations in the distribution from measurement to measurement, it would be possible to substantiate whether a possible lack of stability of the standard at that averaging time was traceable to beam noise.

Fig. 23 shows four plots of $\sigma_y(\tau)$ using the Allan variance of the standards containing the tubes shown in Figs. 9, 11, 16, and 17. The standards were measured against the U.S. Naval Observatory time scale (A.1, mean). Correlation exists between the approximate flicker-floor value and the width around the peak of the velocity distribution for the corresponding tube; wider peaks have higher flicker levels. The width generally increases as the beam cross-section increases. One can make the argument that tubes having optics designed for narrow beam widths (relative to the length between interaction regions) tend to make the center frequency less sensitive to beam noise since all non-uniformities across the width are lowered as the cross-section decreases[5]. Fig. 24 is a plot of $\sigma_y(\tau)$ between NBS-4 and the tube of Fig. 7 which was in a commercial standard showing particularly good stability. The tube was a multiple-beam device.

It should be noted that the width of the distribution around the peak may be an indicator of frequency sensitivity to beam noise. If, however, the beam noise itself is very low, then the beam cross-section may be made large without a sacrifice in stability.

Conclusions

The large number of Cs beam tubes that exists today makes it desirable to look at methods of testing and evaluation. Direct measurement of the velocity distribution is possible for all tubes with Ramsey cavities - and is a helpful diagnostic in characterizing the tube independent of other things. Velocity distributions have been shown of 17 commercial Cs tubes, NBS-4 and NBS-6. The plots are entirely governed by beam optics, and correlation did exist between the width of the distribution around the peak and long-term stability of the frequency standards containing the tube. Subsequent measurements will be made of some of the tubes again to look at ageing effects and other possible correlations.

Acknowledgment

Special thanks to Dr. Gernot Winkler and his staff of the U.S. Naval Observatory for their assistance in many aspects of this work.

References

[1] H. Hellwig, S. Jarvis, Jr., D.J. Glaze, D. Halford, and H.E. Bell, Proc. 27th Annual Symposium on Frequency Control, Fort Monmouth, NJ, 1973.

[2] D.A. Howe, H.E. Bell, and H. Hellwig, Proc. 28th Annual Symposium on Frequency Control, Fort Monmouth, NJ, 1974.

[3] N.F. Ramsey, Molecular Beams, Oxford University Press, 1956.

[4] S. Jarvis, Jr., Metrologia, Vol. 10, pp. 87-98, 1974.

[5] S. Jarvis, Jr., NBS Technical Note 660, 1975.

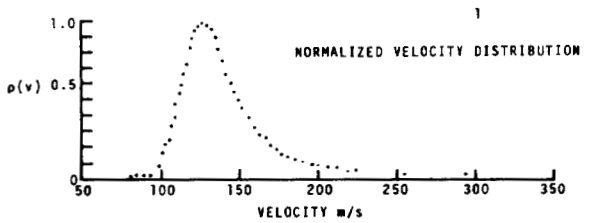

Fig. 2 The Ramsey intensity is measured for a series of selected atomic velocities. The results are normalized to unity.

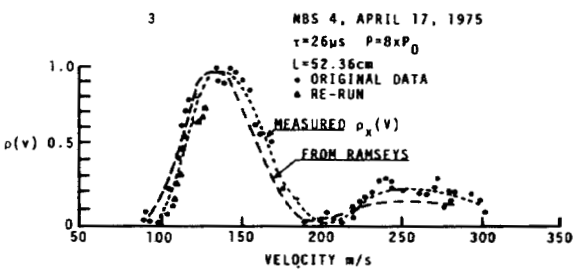

Fig. 4 NBS-4 primary cesium standard with off-axis geometry has a distinct attenuation of atoms at 2 x 10^4 cm/s because of a vane in each R.F. interaction region.

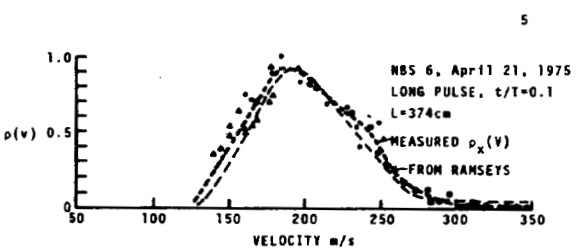

Fig. 5 NBS-6 primary cesium standard incorporates on-axis geometry. A variety of distributions are possible with NBS-6 due to the movable oven and detector.

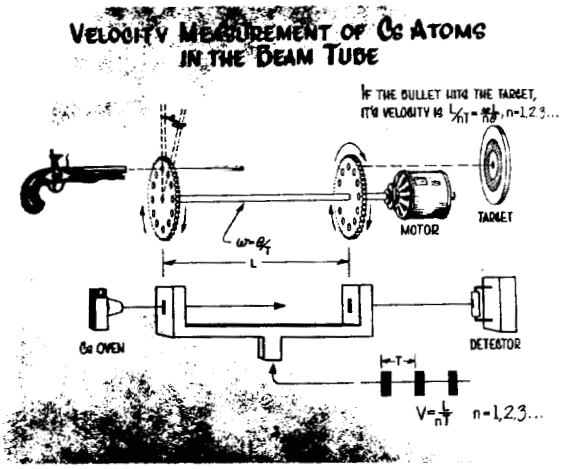

Fig. 1 A mono-velocity mode of operation can be established for a Cs beam tube by making the R.F. excitation signal appear in bursts of prescribed period and width.

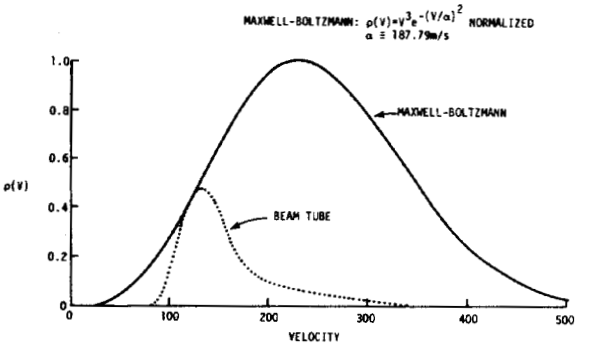

Fig. 3 By comparing a typical beam tube distribution as measured at the detector with the kind of distribution one might see out of the oven, it is evident the beam optics play a major role in determining the contour of the tube's distribution.

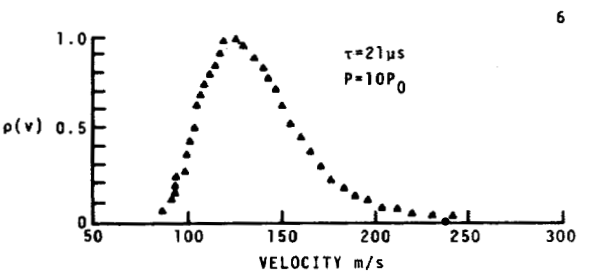

Fig. 6 Commercial tube, single-beam.

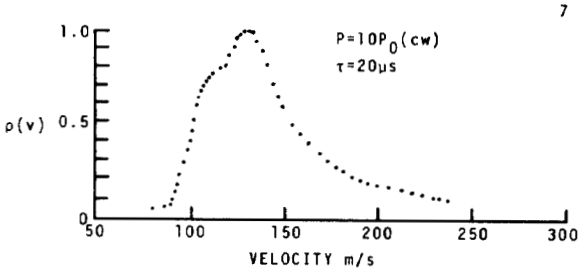

Fig. 7 Commercial tube, multiple-beam.

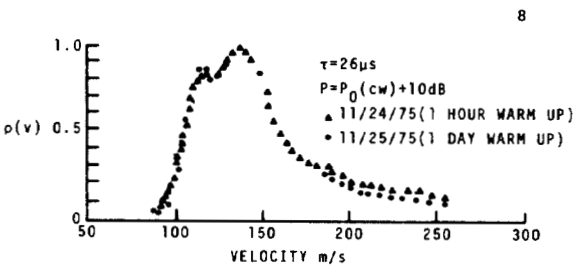

Fig. 8 Commercial tube, multiple-beam.

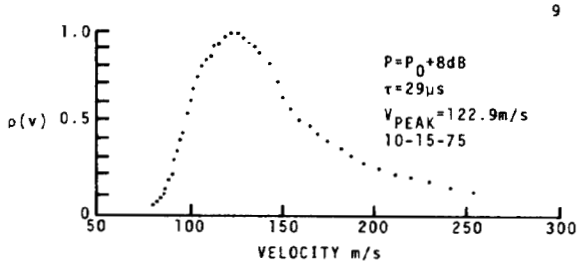

Fig. 9 Commercial tube, single-beam.

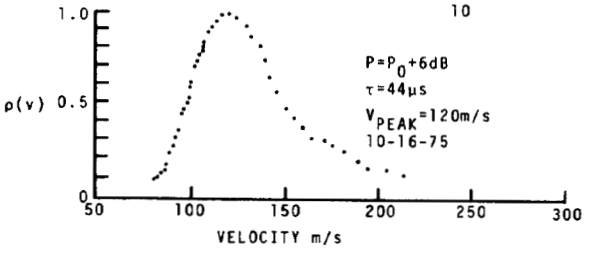

Fig. 10 Commercial tube, single-beam.

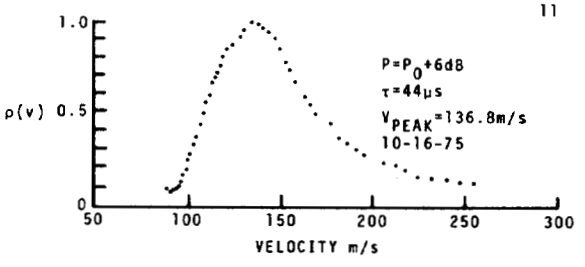

Fig. 11 Commercial tube, multiple-beam.

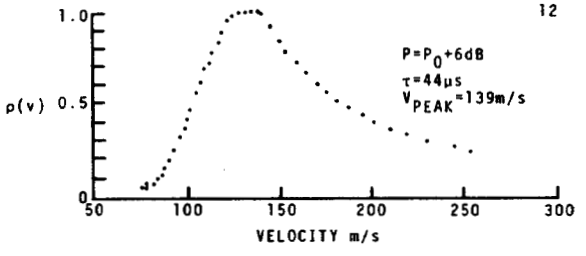

Fig. 12 Commercial tube, single-beam.

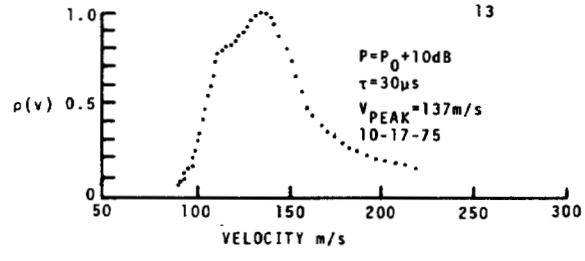

Fig. 13 Commercial tube, multiple-beam.

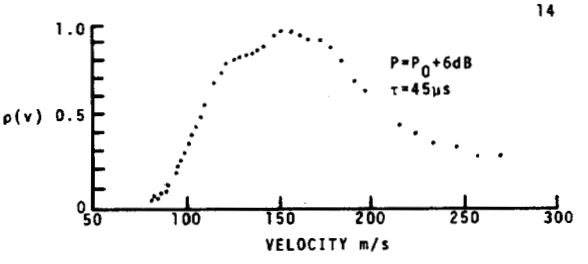

Fig. 14 Malfunctioning commercial tube, single-beam.

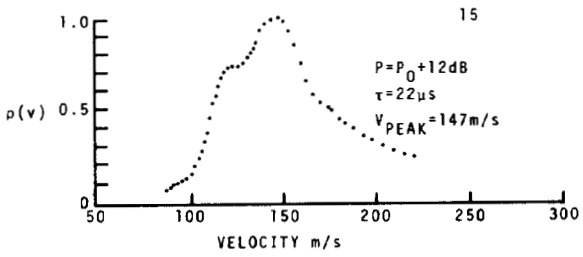

Fig. 15 Commercial tube, multiple-beam.

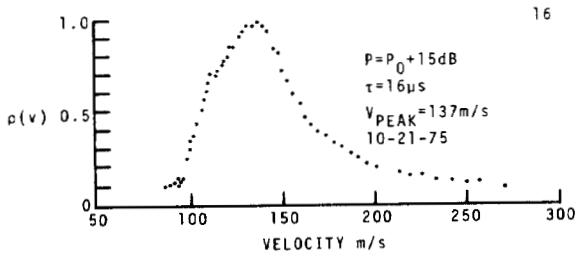

Fig. 16 Commercial tube, multiple-beam.

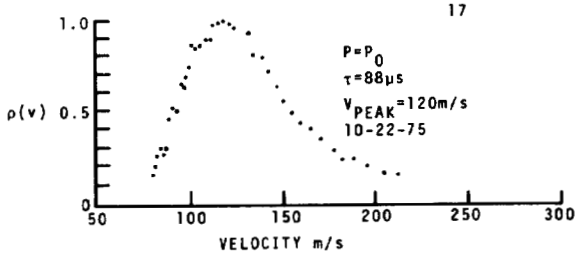

Fig. 17 Commercial tube, single-beam.

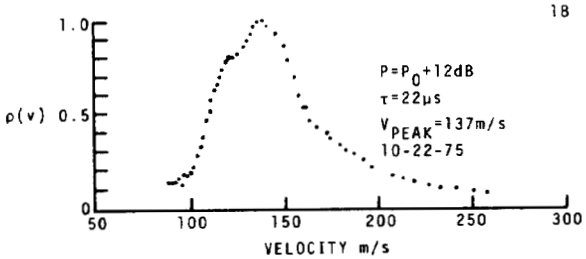

Fig. 18 Commercial tube, multiple-beam.

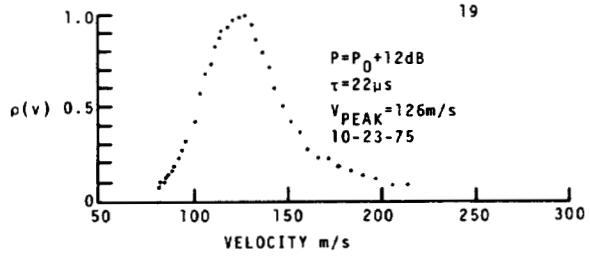

Fig. 19 Commercial tube, single-beam, five year life.

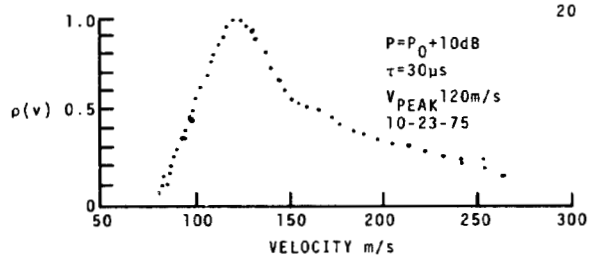

Fig. 20 Commercial tube, single-beam, five year life.

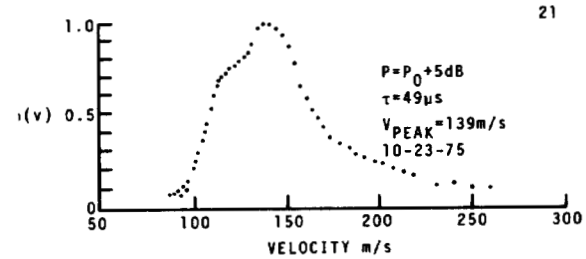

Fig. 21 Commercial tube, multiple-tube, high oven temperature.

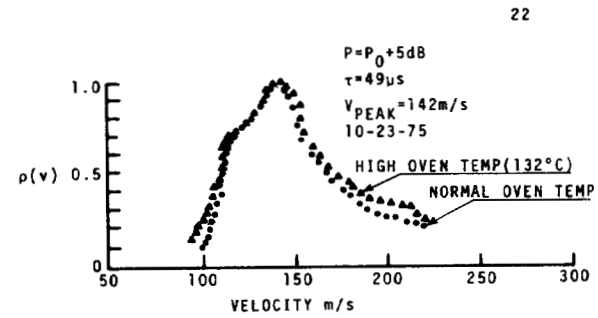

Fig. 22 Commercial tube, multiple-beam, high oven temperature and normal oven temperature.

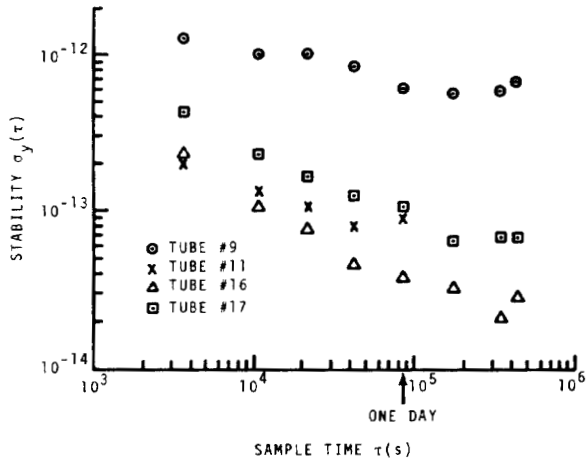

Fig. 23 Plots of frequency stability for standards containing tubes in Figs. 9, 11, 16 and 17. Higher flicker levels seem to go with wider peak feature in velocity distributions for this set of measurements.

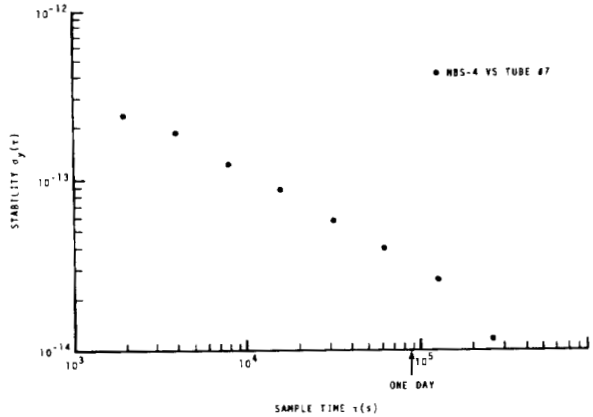

Fig. 24 Plot of frequency stability between NBS-4 and the standard containing the tube of Fig. 7.